J Therm Anal Calorim (2011) 103:229–236
DOI 10.1007/s10973-010-0957-8

Non-isothermal crystallization behaviors of poly(4-methyl-pentene-1)

Shuangjun Chen · Jing Jin · Jun Zhang

Received: 21 December 2009 / Accepted: 5 July 2010 / Published online: 20 July 2010

Abstract Non-isothermal crystallization of isotactic poly-(4-methyl-pentene-1) (P4MP1) is studied by differential scanning calorimeter (DSC), and kinetic parameters such as the Avrami exponent and the kinetic crystallization rate (Z_c) are determined. From the cooling and melting curves of P4MP1 at different cooling rates, the crystalline enthalpy increases with the increasing cooling rate, but the degree of crystalline by DSC measurement shows not much variation. Degree of crystalline of P4MP1 calculated by wide angle X-ray diffraction pattern shows the same tendency with crystalline enthalpy, indicating that re-crystallization occurs when samples heated above the second glass transition temperature of P4MP1. By Jeziorny analysis, n_1 value suggests that mainly spherulites' growth at 2.5 K min^{-1} transforms into a mixture mode of three-dimensional and two-dimensional space extensions with further increasing cooling rate. In the secondary crystallization process, n_2 values indicate that the secondary crystallization is mainly the two-dimensional extension of the lamellar crystals formed during the primary crystallization process. The rates of the crystallization, Z_c and $t_{1/2}$ both increase obviously with the increase of cooling rate, especially at the primary crystallization stage. By Mo's method, higher cooling rate should be required in order to obtain a higher degree of crystallinity at unit crystallization time.

S. Chen · J. Jin · J. Zhang (✉)
Department of Polymer Science and Engineering, College of Materials Science and Engineering, Nanjing University of Technology, Nanjing 210009, People's Republic of China
e-mail: zhangjun@njut.edu.cn

Keywords Poly(4-methyl-pentene-1) · Non-isothermal · Differential scanning calorimeter (DSC) · Crystallization kinetics · Jeziorny analysis · Mo's method

Introduction

Isotactic poly(4-methyl-pentene-1) (P4MP1) exhibits a disordered 7_2 helical conformation in the ordinal crystallite, form I, and these helices form a tetragonal lattice with four chains per unit cell [1]. The polyolefin P4MP1 is known for that the crystal density is lower than the amorphous density at room temperature [2] and atmospheric pressure below 333 K [3]. This special character influences thermal properties and molecular motions of P4MP1. Up to now, many methods, such as mechanical properties [2], Raman analysis [4], small angle X-ray diffraction [5] or X-ray diffraction (XRD) [6, 7], ^{1}H wide line NMR [8], 1D MAS Exchange NMR [9], solid-state ^{13}C MAS NMR [10], and in situ XRD [11, 12] have been applied to characterize thermal properties and molecular motions of P4MP1. Although the structure and properties of P4MP1 crystallized from the bulk have been investigated [13–16], non-isothermal crystallization of P4MP1 has not yet been elucidated.

The crystallization and melting behaviors of polyolefin copolymer [17–23] or homopolymer [24, 25] with short branched chains (SCB) have been intensively investigated recently. During the non-isothermal crystallization process of copolymers, the concentration of random SCB appears as further decisive parameter additionally to the rate of cooling from the melt, because SCB are expelled from crystal lattices [26]; for homopolymers with SCB, the fact that SCB crystallize into crystal lattices makes the SCB lengths play a key role in the crystallization and melting

behaviors [27]. For P4MP1, the special SCB with four carbons endow theoretical and practical significance to study their crystallization kinetics.

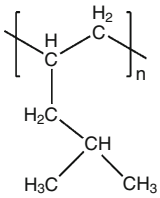

The non-isothermal crystallization behaviors of typical isotactic P4MP1 were investigated by using differential scanning calorimeter (DSC) and wide angle X-ray diffraction (WAXD) in this study. The crystallization kinetics was adequately described via the modified Avrami analysis by Jeziorny and a combination of the Avrami and Ozawa methods developed by Mo. The crystal forms of P4MP1 samples after different cooling rates were discriminated by WAXD.

Experimental

Materials

The polymer, P4MP1, was purchased from Mitsui &Co., Ltd., Japan, and used as-received.

Sample preparation and characterization

Thermal analysis was performed on a Perkin-Elmer DSC-7C DSC under an argon atmosphere. Crystallization behaviors of P4MP1 were investigated at different cooling rates (2.5, 5, 10, 20, 40 K min^{-1}). Melting behaviors were studied by heating the samples after different cooling rates ranging from 333 to 533 K at a step size of 10 K min^{-1}. The degree of crystallinity of P4MP1 (X_c) from DSC was calculated below [28]:

$$X_c = \frac{\Delta H_f}{\Delta H_f^*} \times 100\% \quad (1)$$

where ΔH_f^* is the enthalpy of fusion of the perfect P4MP1 crystal, and ΔH_f is the enthalpy of fusion of P4MP1 measured in DSC. The value of ΔH_f^* for P4MP1 is 117.2 J g^{-1} in literature [28, 29].

Crystal forms of P4MP1 samples after different cooling rates conducted on hot stage (TS1500, Japan) were investigated by WAXD in a Shimadzu XRD-6000 diffractometer (Cu K_α radiation, 40 kV and 30 mA). The scanning angle 2θ ranged from 5° to 50° with the scanning velocity of 4° min^{-1}. The degree of crystallinity of P4MP1 (X_{ca}) from WAXD was calculated as follows [30]:

$$X_{ca} = \frac{A_c}{A_c + A_a} \times 100\% \quad (2)$$

where A_c is the integral area of P4MP1 crystal peak and A_a is the amorphous area of P4MP1 WAXD pattern.

Results and discussion

Non-isothermal crystallization and melting behaviors

DSC traces of P4MP1 at various cooling rates (2.5, 5, 10, 20, 40 K min^{-1}) and the subsequent melting DSC traces are shown in Fig. 1. The detailed data from Fig. 1a are listed in Table 1 and data from Fig. 1b listed in Table 2.

In Fig. 1a and Table 1, five cooling rates (2.5, 5, 10, 20, and 40 K min^{-1}) were used for crystallization of P4MP1. At cooling rate 2.5 K min^{-1}, T_c^{on}, T_c^{p},and T_c^{f}, representing the onset, peak, and finish temperature of exothermic peak

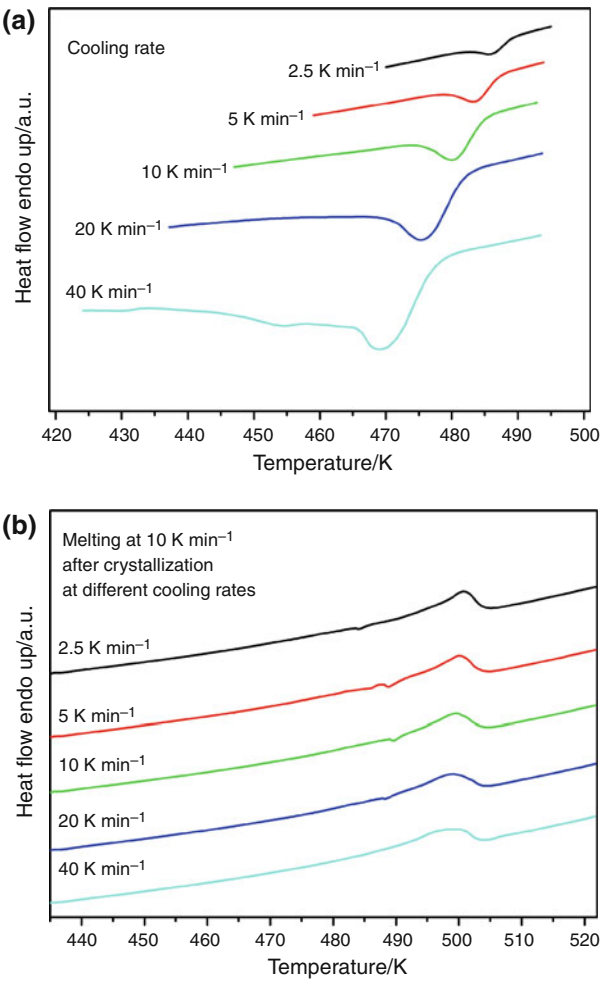

Fig. 1 **a** DSC curves of P4MP1 crystallized at different cooling rates; **b** DSC melting curves at 10 K min^{-1} from 323 to 523 K of P4MP1 crystallized at different cooling rates

Table 1 DSC data of P4MP1 crystallization after different cooling rates

Cooling rate/K min^{-1}	T_c^{on}/K	T_c^{p}/K	T_c^{f}/K	ΔT_c/K	ΔH_c/J g^{-1}
2.5	489.2	486.0	482.3	6.9	9.4
5	487.3	483.6	479.0	8.3	11.7
10	484.9	480.2	475.8	9.1	14.0
20	481.9	475.7	471.0	10.9	13.6
40	477.2	470.3	465.8	11.4	15.3

Table 2 DSC data of melting curves and degree of crystalline (X_c) by WAXD of P4MP1 samples after different cooling rates

Cooling rate/ K min^{-1}	T_m^{p}/K	T_m^{f}/K	ΔH_m/J g^{-1}	X_c/%	X_c/% by WAXD
2.5	500.7	505.2	11.9	10.15	15.22
5	499.9	505.1	12.0	10.24	33.47
10	499.2	505.1	12.1	10.29	38.76
20	498.5	505.1	12.6	10.75	40.72
40	497.8	505.0	12.9	11.00	44.22

are at 489.2, 486.0, and 482.3 K, respectively; at cooling rate 40 K min^{-1}, T_c^{on}, T_c^{p},and T_c^{f} of exothermic peak are at 477.2, 470.3, and 465.8 K, respectively. As cooling rate increases, the crystallization temperature becomes lower obviously. At higher cooling rate the activation of nuclei occurs at lower temperatures, whereas when the samples are cooled at lower scanning rates, crystallization occurs at higher temperatures [31]. Crystallization at lower temperature is unfavorable to the lamellae thickening of P4MP1, because the chain mobility is reduced at lower temperature. So that secondary crystallization appears obvious at cooling rate 40 K min^{-1} and little at cooling rate 2.5 K min^{-1}, which suggests that the secondary crystallization of P4MP1 was the re-arrangement of loose packed chains during the primary crystallization.

ΔT_c in Table 1, the temperature range of crystallization process from T_c^{f} to T_c^{on} becomes larger as the cooling rate increases, which indicates that the crystalline homogeneity decreases [32]. However, special observation in Table 1 is that the crystalline enthalpy ΔH_c has a tendency to increase with the increase in the cooling rate. This phenomenon may be attributed to the two competing factors of nucleation and lamellae thickening during the crystallization process of P4MP1 [26]. As mentioned, crystallization at lower temperature is unfavorable to the lamellae thickening, but favors the nucleation during the crystallization process of P4MP1, because polymer chains achieve more crystallization driving force when crystallized at lower temperature [31]. Therefore, although the crystalline homogeneity decreases with the increase in cooling rate, the crystalline enthalpy is enlarged.

The subsequent melting curves of P4MP1 crystallized after the five cooling rates are shown in Fig. 1b and data derived from Fig. 1b are listed in Table 2. The melting peak temperature, T_m^{p}, of P4MP1 after crystallization decreases with the increase in the cooling rate. For example, T_m^{p} after 2.5 K min^{-1} is 500.7 K, whereas after 40 K min^{-1} reduces to 497.8 K. The above-mentioned homogeneity of P4MP1 crystalline indicated by ΔT_c can be responsible for the change of T_m^{p}. However, T_m^{f}, the finish temperature of melting peak is almost the same, which suggests that the nuclei of P4MP1 is not influenced by the different cooling rates. Crystalline enthalpy ΔH_c is often related with the degree of crystalline. Unlike ΔH_c in Table 1, ΔH_m and X_c in Table 2 are almost the same and have very little increase with the increase in cooling rate. In Fig. 1b, there exist exothermic peaks of re-crystallization in the DSC traces of P4MP1 after 2.5, 5, 10, 20 K min^{-1}. At a same heating rate of 10 K min^{-1}, the re-crystallization makes the X_c almost invariable.

Figure 2 shows the scatter diagram and Lorentz fitting curve of the onset-temperature of non-isothermal crystallization T_c^{on} versus the logarithm of the cooling rate (log Φ) [33]. The curve is not linear regression in the range of cooling rates. By Lorentz fitting, the crystallization temperature T_c^{on} versus cooling rate Φ is formally described by the equation:

$$T_c^{on} = a - b(\log(\Phi) - c)^{-2} \quad (3)$$

where a, b, and c are constants. If Eq. 3 is extended to all the range of cooling rate, the schematic plot is shown as the inset in Fig. 2. The intercept of Y-axis of T_c^{on} is 490.80 K when Φ tends to be zero; T_c^{on} has lowest value 441.72 K in the inset fitting curve. The 500.80 K value means the maximum crystallization temperature above which

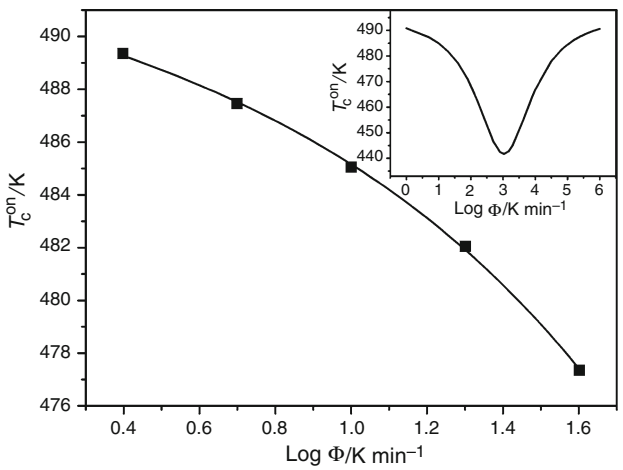

Fig. 2 Onset temperature of non-isothermal crystallization of P4MP1 versus logarithm of cooling rate Φ

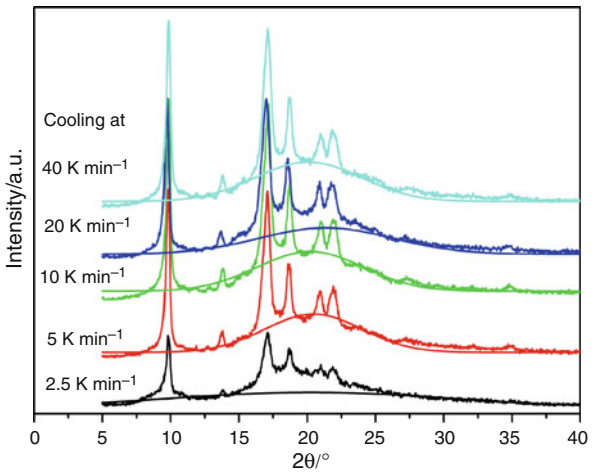

Fig. 3 WAXD patterns of P4MP1 prepared after different cooling rates on hot stage

the P4MP1 will not crystallize during non-isothermal crystallization.

Five different crystalline forms have been found for P4MP1. Among these crystalline forms, form I is the most stable crystalline form which often occurs in melt crystallized samples and in extruded fibers. Form I is characterized by chains in 7_2 helical conformation packed in a tetragonal unit cell [1]. Figure 3 presents the WAXD patterns of P4MP1 prepared at different cooling rates (2.5, 5, 10, 20, 40 K min^{-1}) on hot stage. In Fig. 3, six perceptible diffractive peaks around 9.8°, 17.0°, 18.7°, 20.9°, and 21.9° are relative to typical (200), (220), (311), (212), (400), and (203) crystallographic planes of form I orthorhombic phase, respectively [34]. As cooling rate changes, the crystalline structure has no much variation. So that the WAXD patterns show mainly a modified form I crystalline structure, despite of the cooling rate. The value of $I/I_{\max}$ has a change when cooling rate is 2.5 K min^{-1}. Its peak with maximum diffractive intensity lay at 17.09°, not at around 9.8° like others. This effect may be derived from the above-mentioned complex nucleation when at cooling rate 2.5 K min^{-1}.

In Table 2, there also presents the degree of crystalline X_c calculated by WAXD. In Table 1, the crystalline enthalpy ΔH_c has a tendency to increase with the increase in the cooling rate. However, in Table 2, the degree of crystalline by DSC measurement shows not much variation, which is delusive. Actually, degree of crystalline of P4MP1 by WAXD patterns calculated from Eq. 2 after different cooling rates shows the same tendency with the crystalline enthalpy ΔH_c. As indicted by Danch and Osoba [14, 15], the first glass transition of PMP is about 310–320 K, and this glass transition has not much influence on the non-crystallization behaviors of P4MP2. However, the second transition of P4MP1 is ranged from 350 to 420 K, and this glass transition has a lot of influence on the crystallization behaviors, so that P4MP1 was reported to had unusual thermal behaviors that an equilibrium crystallization occurs on heating [12, 35]. So in the DSC measurements, the re-crystallization of PMP at same heating rate above the second glass transition temperature of PMP in 'semi-ordered' phases made the X_c almost no change.

Non-isothermal crystallization kinetics

The modified Avrami analysis proposed by Jeziorny [36], the Ozawa analysis [37], the Ziabicki analysis [38], and Mo's method [39] have been developed to describe the non-isothermal crystallization kinetics of polymers. The Kissinger method is inapplicable to a process that occurs on cooling, such as the crystallization of polymer melt [40]. In this study, the Jeziorny method [36] and a kinetic model suggested by Mo and coauthors [39] were used to describe the non-isothermal crystallization kinetics of P4MP1. The Ozawa model [37] was not suitable for this study because of the variation in the range of crystallization temperature.

Jeziorny method

The Avrami equation based on the assumption of constant crystallization temperature is given as [41, 42]

$$X_t = 1 - \exp(-Z_t t^n) \tag{4}$$

where n is the Avrami crystallization exponent dependent on the nucleation mechanism and growth dimension, t the time taken during the crystallization process, Z_t the growth rate constant, which depends on nucleation and crystal growth, and X_t is the relative crystallinity [43]. The relative crystallinity, X_t, is defined as follows

$$X_t = \frac{\int_{t_0}^{t} (\mathrm{d}H_c/\mathrm{d}t)\mathrm{d}t}{\int_{t_0}^{t_\infty} (\mathrm{d}H_c/\mathrm{d}t)\mathrm{d}t} \times 100\% \tag{5}$$

where the t_0 and t_∞ represent the time at the onset and the end of the crystallization process, respectively. Using the following equation,

$$t = \frac{T_0 - T}{\Phi} \tag{6}$$

where T is the temperature at crystallization time t, and Φ stands for the cooling rate (2.5, 5, 10, 20, 40 K min^{-1}). The horizontal temperature axis could be transformed into a temperature scale

$$X_T = \frac{\int_{T_0}^{T} (\mathrm{d}H_c/\mathrm{d}T)\mathrm{d}T}{\int_{T_0}^{T_\infty} (\mathrm{d}H_c/\mathrm{d}T)\mathrm{d}T} \times 100\% \tag{7}$$

where T_0 denotes the onset crystallization temperature, T and T_∞ represent the crystallization temperature at time t and

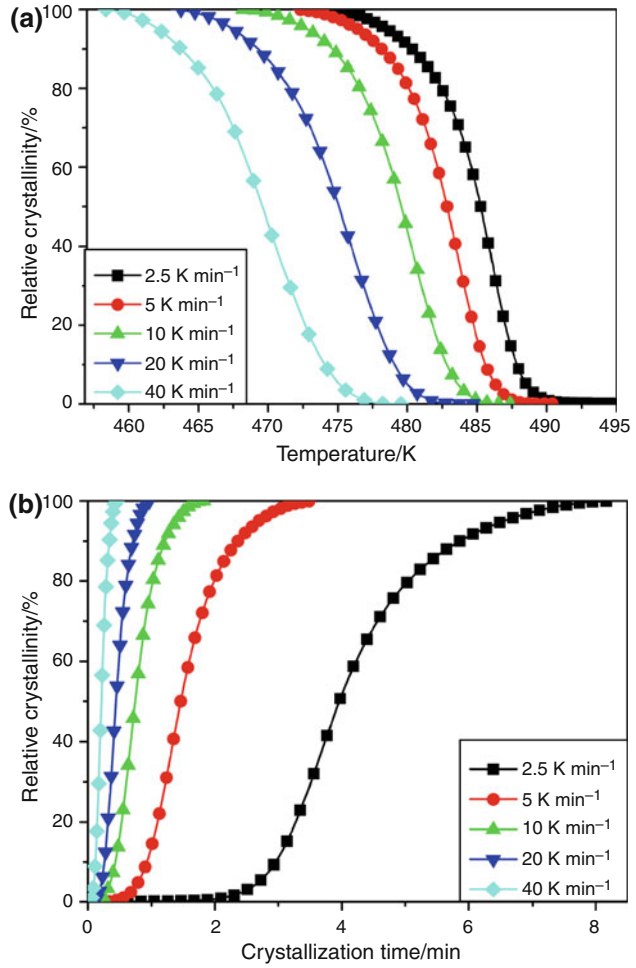

Fig. 4 **a** Plots of relative crystallinity (%) versus temperature; **b** plots of relative crystallinity (%) versus crystallization time for P4MP1 during the non-isothermal crystallization process

after the completion of the crystallization process, respectively. And dH_c stands for the enthalpy of the crystallization released during an infinitesimal temperature range dT [44].

Figure 4a shows the X_T as a function of T for P4MP1. It can be seen that all curves have approximately the same reversed sigmoid shapes. As also observed, the higher the cooling rate, the lower the temperature to initiate the crystallization, indicating there is no enough time to activate nuclei at higher temperatures when crystallized at higher cooling rates. Therefore, nucleation occurs at lower temperatures [43]. The values of T on the X-axis in Fig. 4a can be transformed into crystallization time t according to Eq. 6 as shown in Fig. 4b. All curves have similar sigmoid shapes. Crystallization of P4MP1 occurs at a higher temperature and is completed in a longer time under a lower cooling rate.

The double logarithmic form of Eq. 4 yields

$$\log(-\ln(1 - X_t)) = \log Z_t + n \log t \tag{8}$$

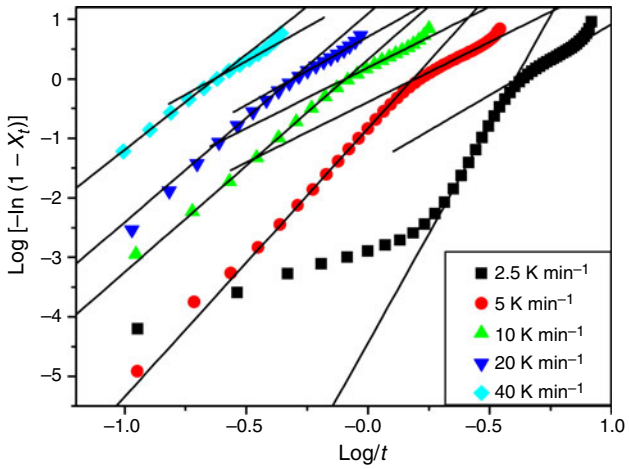

Fig. 5 Plots of $\log(-\ln(1 - X_t))$ versus $\log t$ for P4MP1 during various cooling rate

where X_t is the relative degree of crystallinity, n the Avrami exponent, t the time, and Z_t is the growth-rate constant. Considering the non-isothermal character of the process investigated, Jeziorny suggested that the parameter, Z_t, should be corrected as follows [36]

$$\log Z_c = \log Z_t / \Phi \tag{9}$$

Figure 5 shows the plots of $\log(-\ln(1 - X_t))$ versus $\log t$ for P4MP1. As seen in Fig. 5, all curves are divided into two sections—the primary crystallization stage and the secondary crystallization stage, beside the sample cooling at 2.5 K min^{-1}. The linear lines in the curves are adopted to determine the values of n_1, Z_{t1} at the primary crystallization stage and n_2, Z_{t2} at the secondary crystallization stage from the slope and intercept of the plot, respectively. These parameters with errors are listed in Table 3. Z_{c1}, Z_{c2}, and $t_{1/2}$ are also listed in Table 3.

The value of n is usually an integer varying between 1 and 4, and is dependent on crystallization mechanisms [33]. The n_1 value of P4MP1 at cooling rate 2.5 K min^{-1} is 7.34, which means that it is mainly spherulites' growth with complex nucleation mechanism. As the cooling rate increases, n_1 value decreases to be 3.21 when at cooling rate 40 K min^{-1}. This suggests that as the cooling rate increases, the spherulites' growth transforms into a mixture mode of three-dimensional and two-dimensional space extensions, considering that the nucleation mechanism is homogeneous nucleation [45]. The crystals may grow as small lamellae with lower melting temperature during the non-isothermal crystallization. In the secondary crystallization stage, n_2 values range from 2.02 to 2.38. It is suggested that the dominant secondary crystallization process is by nucleation on preexisting crystals and these secondary crystals are confined to the amorphous regions surrounding

Table 3 Data with errors from Jeziorny method

Cooling rate/K min^{-1}	$n_1 \pm$ Error	$Z_{t1} \pm$ error	Z_{c1}	$n_2 \pm$ Error	$Z_{t2} \pm$ Error	Z_{c2}	$t_{1/2}$/min
2.5	7.34 ± 0.014	(3.71 ± 0.052)e−5	0.017	2.38 ± 0.0060	0.15 ± 0.00039	0.26	3.96
5	4.51 ± 0.0089	(3.34 ± 0.035)e−2	0.68	2.02 ± 0.0046	0.41 ± 0.0017	0.84	1.46
10	3.57 ± 0.018	2.14 ± 0.024	1.08	2.04 ± 0.0063	1.55 ± 0.0025	1.04	0.74
20	3.50 ± 0.031	12.30 ± 0.43	1.13	2.30 ± 0.015	5.13 ± 0.026	1.09	0.44
40	3.21 ± 0.026	104.71 ± 5.19	1.12	2.28 ± 0.014	27.54 ± 0.46	1.09	0.21

the lamellar aggregates [46]. Hence, the n_2 values indicate that the secondary crystallization is mainly the two-dimensional extension of the lamellar crystals formed during the primary crystallization process [47].

In Table 3, $t_{1/2}$ and Z_c values both represent the crystallization rate. The half-time of crystallization, $t_{1/2}$, is defined as the time at which the extent of crystallization is 50%. The greater is the value of $t_{1/2}$, the lower is the rate of the crystallization. It can be seen that $t_{1/2}$ decreases obviously with the increase in cooling rate. In other words, the rate of the crystallization increases obviously with the increase in cooling rate. At the primary crystallization stage, Z_{c1} increases dramatically, while in the secondary crystallization stage, Z_{c2} increases tenderly with the increase in cooling rate. The above observation suggests that undercooling degree may play a key role in the nucleation of P4MP1 which is the control step of the whole crystallization rate [45].

Mo's method

It is evident that in several cases both the Avrami and the Ozawa equations are inadequate in analysis of the non-isothermal crystallization of the polymers. Aiming at finding a method to describe exactly the non-isothermal crystallization process, Mo and coauthors [39] proposed a novel kinetics equation by combining the Avrami and Ozawa equations. Under a certain crystallinity degree, Avrami and Ozawa equations are combined to be

$$\log \Phi = \log[F(T)] - a \log t \tag{10}$$

where the physical meaning of the rate parameter $F(T)$ refers to the necessary value of cooling rate to reach a defined degree of crystallinity at unit crystallization time; a means the a is the ratio of the Avrami exponent n to the Ozawa exponent m, i.e., $a = n/m$. According to Eq. 10, at a given degree of crystallinity, Fig. 6 shows the plot of log $F(T)$ as a function of log t, giving a straight line with log $F(T)$ as the intercept and $-a$ as the slope. The good linearity of the plots verifies the advantage of the combined approach applied in this case. The value of $F(T)$ has a increase systematically with increasing relative crystallinity, indicating that at unit crystallization time, a higher cooling rate should be required in order to obtain a higher degree of crystallinity [32].

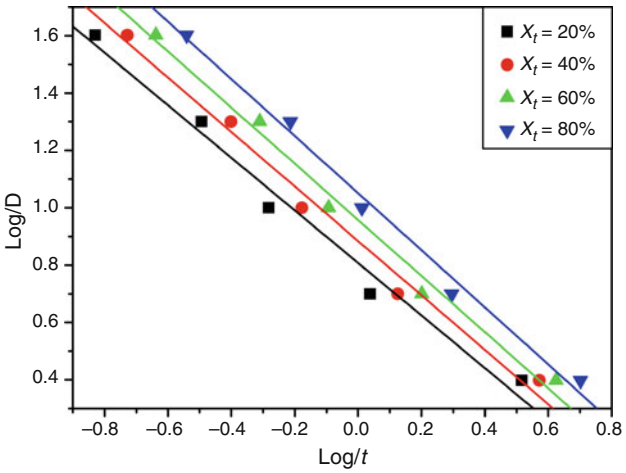

Fig. 6 Plots of log Φ versus log t for P4MP1

Conclusions

From the cooling and melting curves of P4MP1 at different cooling rates, the activation of nuclei occurs at lower temperatures at higher cooling rate; cools at lower scanning rates, crystallization occurs at higher temperatures. Although the crystalline homogeneity decreases with the increase in cooling rate, the crystalline enthalpy increases with the increasing cooling rate. However, the degree of crystalline by DSC measurement shows not much variation. Degree of crystalline of P4MP1 calculated by WAXD patterns shows the same tendency with crystalline enthalpy, indicating that re-crystallization occurs when samples heated above the second glass transition temperature of P4MP1.

Jeziorny analysis and Mo's method are used to investigate the crystallization kinetics of isotactic P4MP1. By Jeziorny analysis, n_1 value suggests that mainly spherulites' growth at 2.5 K min^{-1} transforms into a mixture mode of three-dimensional and two-dimensional space extensions. In the secondary crystallization process, n_2 values indicate that the secondary crystallization is mainly

the two-dimensional extension of the lamellar crystals formed during the primary crystallization process. The rate of the crystallization Z_c increases obviously with the increase in cooling rate, especially at the primary crystallization stage. Undercooling degrees may play a key role in the nucleation of P4MP1 which is the control step of the whole crystallization rate. By Mo's method, at unit crystallization time, a higher cooling rate should be required in order to obtain a higher degree of crystallinity.

References

1. Kusanagi H, Takase M, Chatani Y, Tadokoro H. Crystal structure of isotactic poly(4-methyl-1-pentene). J Polym Sci Polym Phys Ed. 1978;16:131–42.
2. Griffith HJ, Råndy GB. Dilatometric measurements on poly(4-methyl-1-pentene) glass and melt transition temperatures, crystallization rates, and unusual density behavior. J Polym Sci. 1960;44:369–81.
3. Rastogi S, Newman M, Keller A. Unusual pressure-induced phase behavior in crystalline poly-4-methyl-pentene-1. J Polym Sci B Polym Phys. 1993;31:125–39.
4. Samuel EJJ, Mohan S. FTIR and FT Raman spectra and analysis of poly(4-methyl-1-pentene). Spectrochim Acta A. 2004;60:19–24.
5. Tanigami T, Miyasaka K. Small-angle x-ray scattering of isotactic poly(4-methyl-1-pentene). J Polym Sci Polym Phys Ed. 1981;19:1865–71.
6. Tanigami T, Yamaura K, Matsuzawa S, Miyasaka K. Thermal expansion of crystal lattice of isotactic poly(4-methyl-1-pentene). Polym J. 1986;18:35–40.
7. Reddy S, Desai P, Abhiraman SA, Beckham WH, Kulik SA, Spiess WH. Structure and temperature-dependent properties of poly (4-methyl-1-pentene) fibers. Macromolecules. 1997;30:3293–301.
8. Chan SK, Råndy G, Brumberger H, Odajima A. NMR measurements on isotactic poly(4-methyl-1-pentene). J Polym Sci. 1962;61: S29–32.
9. Miyoshi T, Pascui O, Reichert D. Helical jump motions in isotactic poly(4-methyl-1-pentene) crystallites revealed by 1D MAS exchange NMR spectroscopy. Macromolecules. 2002;35:7178–81.
10. Miyoshi T, Pascui O, Reichert D. Slow chain dynamics in isotactic-poly(4-methyl-1-pentene) crystallites near the glass transition temperature characterized by solid-state C-13 MAS exchange NMR. Macromolecules. 2004;37:6460–71.
11. Rastogi S, Newman M, Keller A. Pressure-induced amorphization and disordering on cooling in a crystalline polymer. Nature. 1991;353:55–7.
12. Rastogi S, Hohne GWH, Keller A. Unusual pressure-induced phase behavior in crystalline poly(4-methylpentene-1): calorimetric and spectroscopic results and further implications. Macromolecules. 1999;32:8897–909.
13. Danch A, Osoba W. Structural relaxation of the constrained amorphous phase in the glass transition zone. J Therm Anal Calorim. 2003;72:641–50.
14. Danch A, Osoba W. The nature of the amorphous phase in resultant engineering products. J Mater Process Technol. 2004;155–156: 1428–34.
15. Danch A, Osoba W. Thermal analysis and free volume study of polymeric supermolecular structures. J Therm Anal Calorim. 2004;78:923–32.
16. Danch A, Osoba W. Stability of supermolecular structure below Tg. J Therm Anal Calorim. 2006;84:79–83.
17. Seguela R, Rietsch F. On the isomorphism of ethylene/alpha-olefin copolymers. J Polym Sci C Polym Lett. 1986;24:29–33.
18. Bensason S, Minick J, Moet A, Chum S, Hiltner A, Baer E. Classification of homogeneous ethylene-octene copolymers based on comonomer content. J Polym Sci B Polym Phys. 1998;34:1301–15.
19. Kim MH, Phillips PJ. Nonisothermal melting and crystallization studies of homogeneous ethylene/alpha-olefin random copolymers. J Appl Polym Sci. 1998;70:1893–905.
20. Alizadeh A, Richardson L, Xu J, McCartney S, Marand H, Cheung YW, Chum S. Influence of structural and topological constraints on the crystallization and melting behavior of polymers. 1. Ethylene/1-octene copolymers. Macromolecules. 1999;32:6221–35.
21. Liu JP, Zhang FJ, Fu Q, Liu TB. Influence of short chain branches on crystallization and melting behaviors of low molecular weight polyethylenes. Acta Polym Sin. 2001;4:228–31.
22. Liu JP, He TB. Structure, morphology and melting behaviors of metallocene-catalyzed branched polyethylene. Chin J Polym Bull. 2002;3:52–7.
23. Somrang N, Nithitanakul M, Grady BP, Supaphol P. Non-isothermal melt crystallization kinetics for ethylene-acrylic acid copolymers and ethylene-methyl acrylate-acrylic acid terpolymers. Eur Polym J. 2004;40:829–38.
24. Di Lorenzo ML, Righetti MC. The three-phase structure of isotactic poly(1-butene). Polymer. 2008;49:1323–31.
25. Coppola S, Acierno S, Grizzuti N, Vlassopoulos D. Viscoelastic behavior of semicrystalline thermoplastic polymers during the early stages of crystallization. Macromolecules. 2006;39:1507–14.
26. Kolesov IS, Androsch R, Radusch HJ. Non-isothermal crystallization of polyethylenes as function of cooling rate and concentration of short chain branches. J Therm Anal Calorim. 2004;78: 885–95.
27. Gupta P, Wilkes GL, Sukhadia AM, Krishnaswamy RK, Lamborn MJ, Wharry SM, Tso CC, DesLauriers PJ, Mansfield T, Beyer FL. Does the length of the short chain branch affect the mechanical properties of linear low density polyethylenes? An investigation based on films of copolymers of ethylene/1-butene, ethylene/1-hexene and ethylene/1-octene synthesized by a single site metallocene catalyst. Polymer. 2005;46:8819–37.
28. Brandrup J, Immergut EH. Polymer handbook. New York: Wiley; 1999. p. 736–40.
29. Cornelia Vasile C, Seymour RB. Handbook of polyolefins—synthesis and properties. New York: Marcel Dekker, Inc.; 1993.
30. Stribeck N, Interpretation of scattering patterns. In X-ray scattering of soft matter. New York: Springer; 2007. p. 103–5.
31. Di Lorenzo ML, Silvestre C. Non-isothermal crystallization of polymers. Prog Polym Sci. 1999;24:917–50.
32. Zhang J, Chen SJ, Su J, Shi XM, Jin J, Wang XL, Xu ZZ. Non-isothermal crystallization kinetics and melting behavior of EAA with different acrylic acid content. J Therm Anal Calorim. 2009;97:959–67.
33. Islam MA, Hussein IA, Atiqullah M. Effects of branching characteristics and copolymer composition distribution on non-isothermal crystallization kinetics of metallocene LLDPEs. Eur Polym J. 2007;43:599–610.
34. Charlet G, Delmas G. Effect of solvent on the polymorphism of poly(4-methylpentene-1): 2. Crystallization in semi-dilute solutions. Polymer. 1984;25:1619–25.
35. Rastogi S, Vega JF, van Ruth NJL, Terry AE. Non-linear changes in the specific volume of the amorphous phase of poly (4-methyl-1-pentene); Kauzmann curves, inverse melting, fragility. Polymer. 2006;47:5555–65.
36. Jeziorny A. Parameters characterizing the kinetics of the non-isothermal crystallization of poly(ethylene terephthalate) determined by DSC. Polymer. 1978;19:1142–4.
37. Ozawa T. Kinetics of non-isothermal crystallization. Polymer. 1971;12:150–8.

38. Ziabicki A. Theoretical analysis of oriented and non-isothermal crystallization – 2. Extension of the Kolmogoroff-Avrami-Evans theory onto processes with variable rates and mechanisms. Colloid Polym Sci. 1974;252:433–47.
39. Liu TX, Mo ZS, Wang SG, Zhang HF. Nonisothermal melt and cold crystallization kinetics of poly(aryl ether ether ketone ketone). Polym Eng Sci. 1997;37:568–75.
40. Vyazovkin S. Is the Kissinger equation applicable to the processes that occur on cooling? Macromol Rapid Commun. 2002;23:771–5.
41. Avrami M. Kinetics of phase change. I. General theory. J Chem Phys. 1939;7:1103–12.
42. Avrami M. Kinetics of phase change. II. Transformation-time relations for random distribution of nuclei. J Chem Phys. 1940;78:212–24.
43. Wunderlich B. Macromolecular physics. New York: Academic Press; 1976. p. 147.
44. Cebe P, Hong SD. Crystallization behaviour of poly(ether-ether-ketone). Polymer. 1986;27:1183–92.
45. Wunderlich B. Thermal characterization of polymeric materials. 2nd ed. New York: Academic Press; 1997.
46. Akpalu Y, Kielhorn L, Hsiao BS, Stein RS, Russell TP, van Egmond J, Muthukumar M. Structure development during crystallization of homogeneous copolymers of ethene and 1-octene: time-resolved synchrotron X-ray and SALS measurements. Macromolecules. 1999;32:765–70.
47. Strobl GR, Engelke T, Maderek EUG. On the kinetics of isothermal crystallization of branched polyethylene. Polymer. 1983;24:1585–9.